

1 **SUPPLEMENTARY MATERIALS**

2
3
4
5
6
7
8
9
10
11
12
13
14
15
16
17
18
19
20
21
22
23
24
25
26
27
28
29
30
31
32
33

**Mechanisms of Qingyi decoction in Severe Acute Pancreatitis-
Associated Acute Lung Injury via Gut Microbiota: Targeting Short-
Chain Fatty Acids mediated AMPK/NF-κB/NLRP3 pathway**

Zhengjian Wang,^{a,b,c,#} Jin Liu,^{a,b,c,#} Fan Li,^{a,b,c} Shurong Ma,^{a,c} Liang Zhao,^{a,b} Peng
Ge,^{a,b,c} Haiyun Wen,^{a,b,c} Yibo Zhang,^{a,b,c} Xiaojun Liu,^{b,c,d} Yalan Luo,^{a,b,c} Jiaqi Yao,^{b,c,d}
Guixin Zhang,^{a,b,c,*} Hailong Chen,^{a,c,*}

34 SUPPLEMENTARY METHODS

35 Firstly, the ingredients of the QYD monomer were obtained (Rhubarb, Paeoniae Radix
36 Alba, Radix Bupleuri, Scutellaria baicalensis Georgi, Radix Aucklandiae, Gardenia
37 jasminoides) in Traditional Chinese Medicine Systems Pharmacy Database and Analysis
38 Platform (TCMSP) (<http://LSP.nwu.edu.cn/tcmsp.php>), and the active ingredients were
39 filtered according to the two indicators, namely oral bioavailability (greater than 30%)
40 and drug-likeness (greater than 0.18) [1, 2]. SCFAs-related genes were obtained from the
41 Genecards (www.genecards.org/), and then the dataset GSE194331 (including the
42 transcriptome sequencing data of peripheral blood PBMCs of 32 control subjects and 10
43 SAP patients) was downloaded from GEO. Then, a total of 8154 differential genes were
44 screened (according to $\log_{2}FC > 0.1$ and $adj.P.Val < 0.05$), and these genes were regarded
45 as SAP-related genes [3]. The top 20 up-regulated and down-regulated genes of the
46 differential genes were included in the heatmap using the R pheatmap package to
47 visualize the expression levels of these genes. In the meantime, the R ggplot, ggrepel, and
48 dplyr packages were used to obtain a volcano map. Perl (ActivePerl, version 5.24) was
49 used to convert the active components of monomers into related target genes based on
50 the UniProt database (<http://www.uniprot.org/>). A Venn diagram was drawn by R
51 package, and 14 common genes were obtained by intersecting the SAP-related genes,
52 SCFAs gene, and the target genes of SCFAs corresponding to each monomer. Next,
53 Cytoscape v3.9.0 (www.cytoscape.org/) was used to draw a network regulation map of
54 SAP-QYD-SCFAs-related genes [4]. Finally, a gene function enrichment analysis was

55 performed based on Gene Ontology (GO) and the Kyoto Encyclopedia of Genes and
56 Genomes (KEGG), and then the R ggplot2 package was used for bubble charts for
57 visualization.

58

59

60

61

62

63

64

65

66

67

68

69

70

71

72

73

74

75

76

77

78

79

80

81

82

83

84

85

86

87

Table S1. The pathological score criteria of pancreas.

Condition	Score	Description
Edema	0	Absent
	1	Diffuse expansion of interlobar septae
	2	Same as 1 + diffuse expansion of interlobular septae
	3	Same as 2 + diffuse expansion of interacinar septae
	4	Same as 3 + diffuse expansion of intercellular spaces
Inflammation and perivascular infiltrate	0	0-1 intralobular or perivascular leukocytes/ HPF
	1	6-10 intralobular or perivascular leukocytes/ HPF
	2	16-20 intralobular or perivascular leukocytes/ HPF
	3	26-30 intralobular or perivascular leukocytes/ HPF
	4	>35 leukocytes/HPF or confluent microabscesses
Hemorrhage and fat necrosis	0	Absent
	1	2 foci
	2	4 foci
	3	6 foci
	4	8 foci
Acinar necrosis	0	Absent
	1	Diffuse occurrence of 1-4 necrotic cells/HPF
	2	Diffuse occurrence of 5-10 necrotic cells/HPF
	3	Diffuse occurrence of 11-16 necrotic cells/HPF (Foci of confluent necrosis)
	4	> 16 necrotic cells/HPF (Extensive confluent necrosis)

89

90

91

92

93

94

95

96

97

98

99

100

101

102

103

Table S2. The pathological score criteria of intestine.

Grade	Pathologic score
0	Normal mucosal villi
1	Development of subepithelial Gruenhagen's space at the apex of the villus
2	Extension of the subepithelial space with moderate lifting of the epithelial layer from the lamina propria
3	Massive epithelial lifting down the sides of villi, possibly with a few denuded tips
4	Denuded villi with the lamina propria and dilated capillaries exposed
5	Digestion and disintegration of the lamina propria, hemorrhage, and ulceration

104

105

106

107

108

109

110

111

112

113

114

115

116

117

118

119

120

121

122

123

124

125

126

127

128

129

130

131

132

Table S3. The pathological score criteria of lungs.

Condition	Score	Description
Neutrophil Infiltration	0	No or very mild
	1	Mild
	2	Moderate
	3	Severe
	4	Very severe
Edema	0	No or very mild
	1	Mild
	2	Moderate
	3	Severe
	4	Very severe
Disorganization Of Lung Parenchyma	0	No or very mild
	1	Mild
	2	Moderate
	3	Severe
	4	Very Severe
Hemorrhage	0	No or very mild
	1	Mild
	2	Moderate
	3	Severe
	4	Very severe

134

135

136

137

138

139

140

141

142

143

144

145

146

147

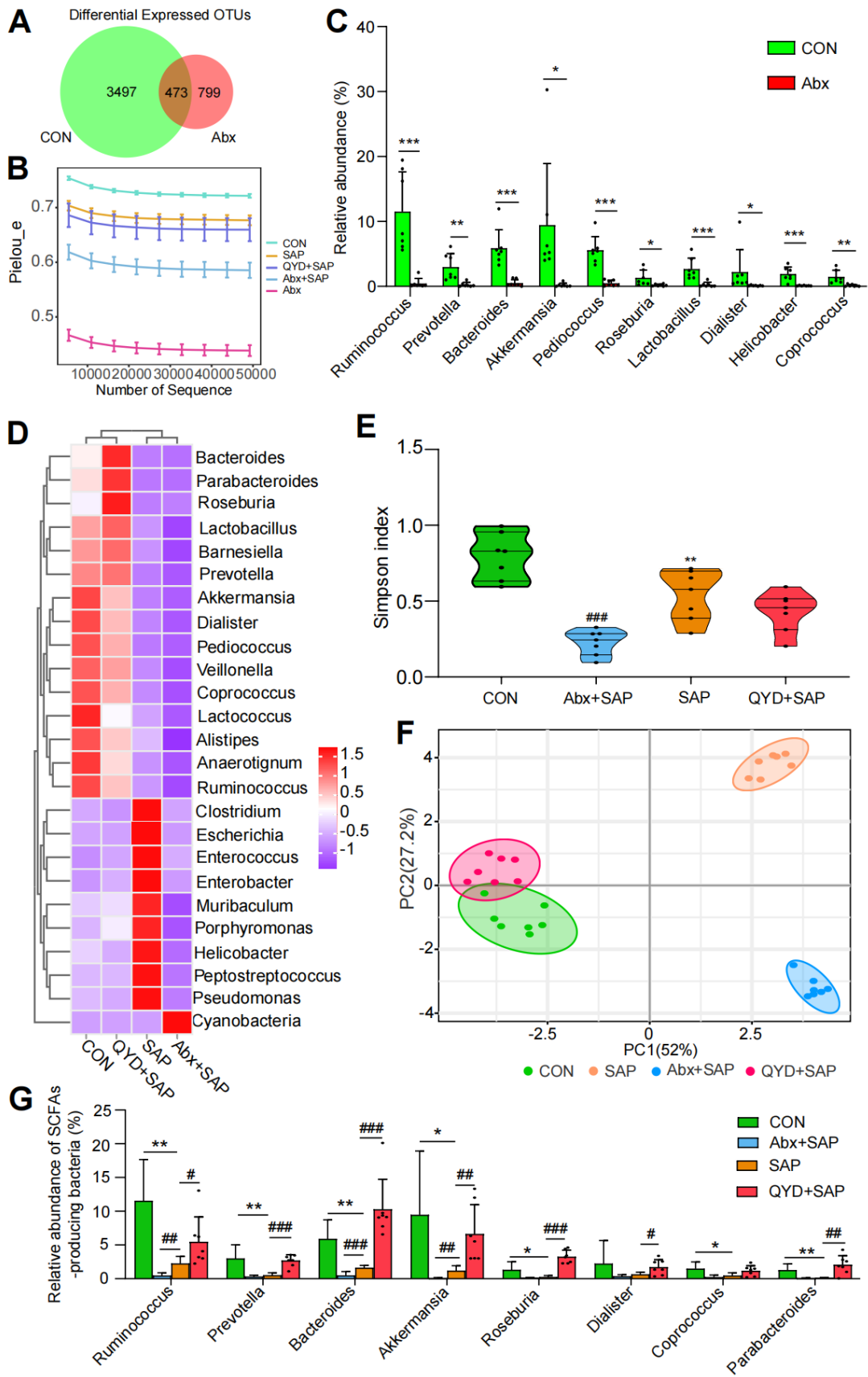
148

149

150

151

152



154 **Figure S1. The composition and diversity analysis results of gut microbiota based**
155 **on 16S rDNA sequencing.** (A) Venn diagram of the CON and Abx groups based on
156 OTU abundance. The numbers represent the values of OTUs that can be detected in all
157 mice in a group. (B) Sparsity curves based on the pielou-e index showing species
158 richness of each group. (C) The histogram shows the difference in the relative
159 abundance of the TOP 10 genera between the CON and Abx groups. (D) Clustering
160 heatmaps of bacteria at genus level in different groups. (E) Alpha diversity analysis of
161 intestinal bacteria at the genus level (Simpson index). (F) PCA plot based on weighted
162 unifrac distance matrix analysis of top25 bacteria. (G) The histogram shows the
163 differences in the major SCFAs-producing genera in each group. Data are shown as
164 mean \pm SEM (n=7 per group) and analyzed by unpaired student's t-test with *, $P < 0.05$;
165 **, $P < 0.01$; ***, $P < 0.001$ in comparison with the CON group and #, $P < 0.05$; ##, P
166 < 0.01 ; ###, $P < 0.001$ in comparison with the SAP group.

167

168

169

170

171

172

173

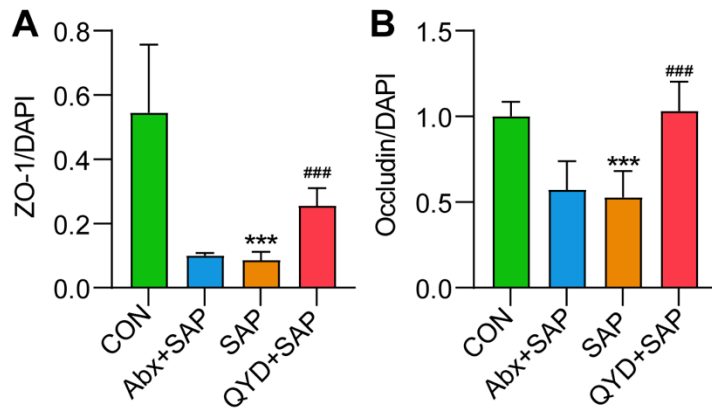
174

175

176

177

178



179

180 **Figure S2. Semiquantitative results of tight junction protein in intestine. (A)**

181 Relative expression ratio of ZO-1/DAPI. (B) Relative expression ratio of

182 occludin/DAPI. Data are shown as mean \pm SEM (n=7 per group) and analyzed by

183 unpaired student's t-test with ***, $P < 0.001$ in comparison with the CON group and

184 ###, $P < 0.001$ in comparison with the SAP group.

185

186

187

188

189

190

191

192

193

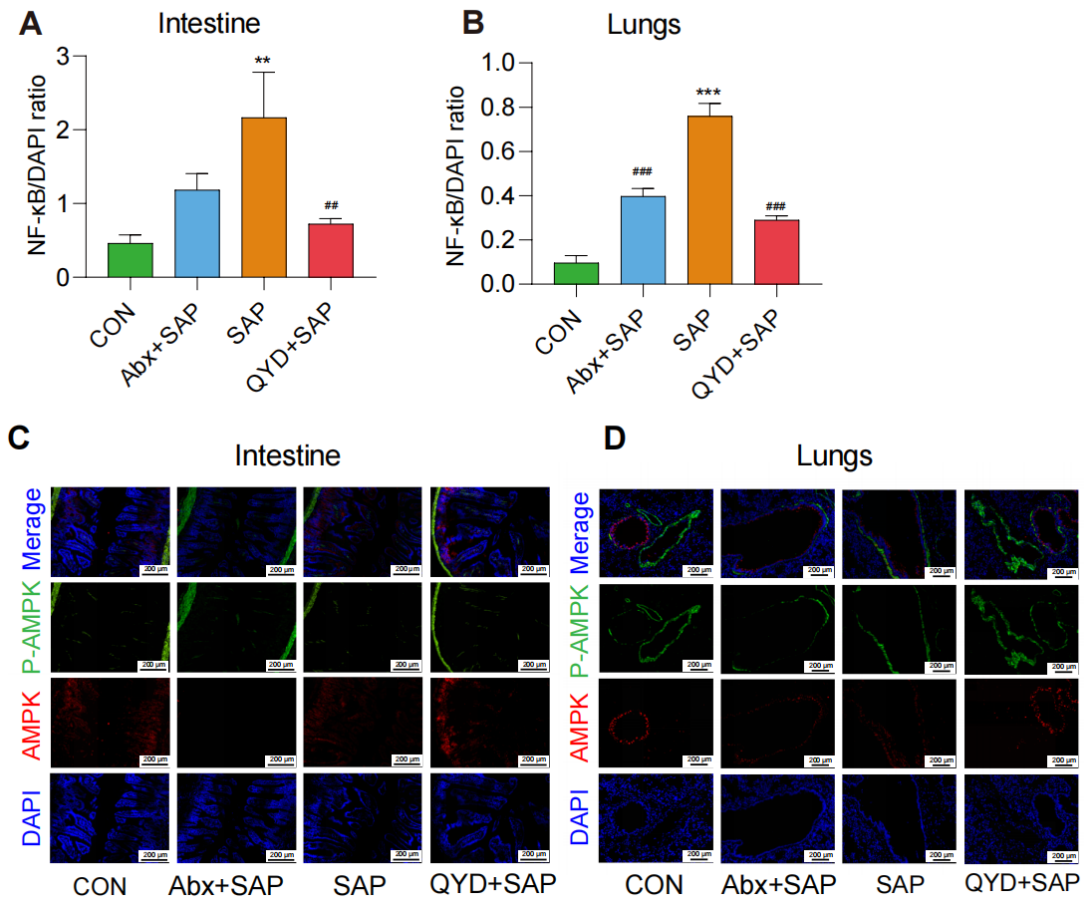
194

195

196

197

198



199

200 **Figure S3. Semiquantitative results of NF-κB and immunofluorescence staining of**

201 **AMPK-related proteins.** (A) Relative expression ratio of NF-κB/DAPI in the intestine.

202 (B) Relative expression ratio of NF-κB/DAPI in lungs. (C-D) Immunofluorescence

203 staining results of AMPK (in red), p-AMPK (in green), DAPI (in blue), and the merge

204 images, scale bar: 100 μm in lungs, and 200 μm in the intestine. Data are representative

205 images with at least three independent experiments and analyzed by unpaired student's

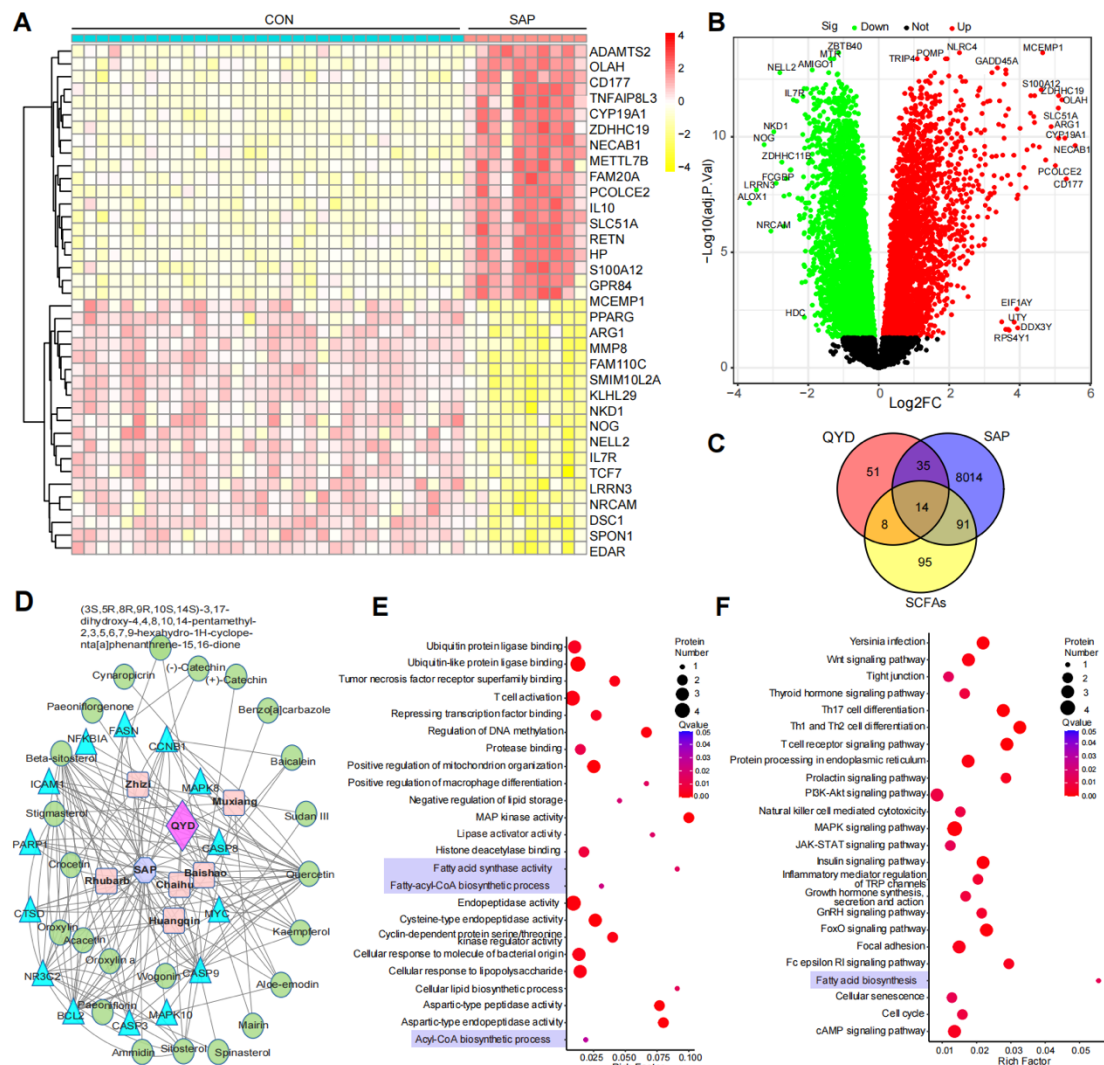
206 t-test. ***P* < 0.01; ****P* < 0.001 in comparison with the CON group and ##*P* < 0.01;

207 ###*P* < 0.001 in comparison with the SAP group.

208

209

210



211

212 **Figure S4. Relationship between QYD treatment and the major components of**
 213 **SCFAs in SAP patients based on network pharmacology. (A) Clustering heatmap of**

214 **the up-regulated and down-regulated TOP20 genes in SAP patients and control subjects**

215 **based on the GSE194331 dataset. (B) The volcano plot shows the differential genes**

216 **between SAP patients and control subjects based on the GSE194331 dataset, according**

217 **to the absolute value of log₂FC. The log₂FC value above 0.1 and P value less than 0.05**

218 **was set as the limit, and the most significant differential genes were marked with**

219 **symbolic names. (C) The Venn diagram of the intersection of target genes in response to**

220 **active ingredients of QYD, SAP-related genes, and SCFAs-related genes (acquired by**

221 Genecards), obtaining a total of 14 intersecting genes. (D) Network map showing the
222 SAP-related genes, target genes in response to QYD active ingredients, and SCFAs-
223 related genes (acquired by Genecards). (E) Visualized bubble plot for functional
224 enrichment analysis of intersecting genes based on the Gene Ontology (GO) database. (F)
225 Bubble plot for functional enrichment analysis of intersecting genes based on the Kyoto
226 Encyclopedia of Genes and Genomes (KEGG) database. Latin name: Zhizi, *Gardenia*
227 *jasminoides*; Muxiang, *Radix Aucklandiae*; Chaihu, *Radix Bupleur*; Baishao, *Paeoniae*
228 *Radix Alba*; Huangqin, *Scutellaria baicalensis* Georgi.

229

230

231

232

233

234

235

236

237

238

239

240

241

242

243

244

245

246

247

248

249

250

251

252

253

254

255

256

257 **REFERENCES**

- 258 1. Ru J, Li P, Wang J, Zhou W, Li B, Huang C, et al. TCMSP: a database of systems
259 pharmacology for drug discovery from herbal medicines. *J Cheminform* (2014)
260 6:13. doi: 10.1186/1758-2946-6-13.
- 261 2. Zhang W, Chen Y, Jiang H, Yang J, Wang Q, Du Y, et al. Integrated strategy for
262 accurately screening biomarkers based on metabolomics coupled with network
263 pharmacology. *Talanta* (2020) 211:120710. doi: 10.1016/j.talanta.2020.120710.
- 264 3. Chen S, Sun Z, Deng W, Li G, Liu X, Zhang Z. Whole transcriptome analysis of
265 long noncoding RNA in beryllium sulfate-treated 16HBE cells. *Toxicol Appl*
266 *Pharmacol* (2022) 449:116097. doi: 10.1016/j.taap.2022.116097.
- 267 4. Piñero J, Saüch J, Sanz F, Furlong LI. The DisGeNET cytoscape app: Exploring
268 and visualizing disease genomics data. *Comput Struct Biotechnol J* (2021)
269 19:2960-7. doi: 10.1016/j.csbj.2021.05.015.